*Experimental and Computational Multiphase Flow*
Vol. 2, No. 1, 2020, 41–51
https://doi.org/10.1007/s42757-019-0022-1

# Visualization and measurement of two-phase flows in horizontal pipelines

**Paolo Sassi (✉), Jordi Pallarès, Youssef Stiriba**

*Departament d'Enginyeria Mecànica, Universitat Rovira i Virgili, 43007-Tarragona, Spain*

## Abstract

Understanding the dynamics of gas–liquid two-phase flows (G/L), is crucial to predict the transport efficiency of the mixture and the energy needed for pumping. In addition, many industrial processes are governed by momentum, heat, and mass transfer phenomena between the phases. Many examples can be found in the different stages of refinement up to the production of petroleum products, biomass transport, chemical reactors, nuclear waste decommissioning, pulp, and paper production, among many others.

In this study, an experimental facility designed to analyze G/L mixture is presented and discussed. The experimental results are presented for gas–liquid flows in horizontal 30 mm ID pipelines. The mixture involved is composed of air and water. The superficial velocity of the liquid phase is in the range of 0–2 m/s and the gas phase from 0 to 2 m/s.

The experimental data accounts for pressure loss, hold-up, superficial velocities, and flow regimes. A flow map is presented covering the specified ranges, and two-phase correlations for hold-up and frictional pressure loss are reported and compared with the available experimental data.

## Keywords

two-phase flows
experimental analysis
frictional pressure drop
void fraction

## Article History

Received: 26 February 2019
Revised: 2 April 2019
Accepted: 3 April 2019

## Research Article



## 1 Introduction

Two-phase flows are any kind of flow involving two phases delimited by an interface. This includes a wide spectrum of flows, that encompasses liquid–liquid immiscible flows, gas–liquid, gas–solid and liquid–solid. The analysis and characterization of two-phase G/L mixtures flowing in pipes are essential for some global industry sectors, specially the oil, nuclear, and chemical industries (Beggs and Brill, 1973). The key parameters to characterize G/L mixture flows are:

(1) The flow regime. This is the spatial distribution of the phases inside the pipe. Mandhane et al. (1974) were the first ones to propose a flow regime map. However, no specific influence on the pipe size was reported until the work of Taitel and Dulker (1976). They have suggested that, in the case of larger pipe diameters, the bubbly to plug and the plug/slug to stratified boundaries move to higher values of liquid superficial velocities, and that the stratified to annular transition boundary moves towards a higher gas superficial velocity.

(2) The pressure drop. One of the seminal works regarding multiphase flows was carried out by Lockhart and Martinelli (1949). They developed a correlation to calculate the frictional pressure gradient (FPG) of liquid–gas mixtures in horizontal pipelines. The L–M correlation has been used both in the industry and in many research studies, mainly because of its simplicity and its ability to predict reliably the pressure drop. Since their study, several authors have validated such correlation (Dukler et al., 1964; Mao et al., 1997; Abduvayt et al., 2003). In particular, Chisholm (1967) has proposed a simplified correlation with a theoretical basis.

(3) The void fraction, or hold-up, can determine the gas distribution along pipelines and the interfacial area concentration, which results of great importance for several chemical processes, because they are usually governed by momentum, heat, and mass transfer phenomena between the phases. Beggs and Brill (1973) have proposed a correlation that determines the FPG and the void fraction for air–water mixtures in pipelines at any inclination angle. In order to measure the void fraction, they used pneumatically actuated, quick-closing ball valves. By closing simultaneously two separated valves, they measured the void fraction of the trapped mixture between the valves.

This work aims to analyze two-phase flows inside

✉ paolo.sassi@urv.cat

## Nomenclature

*Variables*

| | |
|---|---|
| $C$ | Auxiliar parameter for correlations |
| $C_o$ | Distribution parameter (drift flux model) |
| $D$ | Internal diameter of pipeline (m) |
| $f$ | Darcy–Weisbach friction factor |
| $Fr$ | Froude number |
| $g$ | Acceleration of gravity, 9.81 m/s$^2$ |
| $H$ | Hold-up |
| $j$ | Superficial velocity (m/s) |
| $Lv$ | Liquid velocity number, $= j_f \cdot (\rho_f / \rho_g)^{0.25}$ |
| $P$ | Pressure (Pa) |
| $Q$ | Flow rate (m$^3$/s) |
| $Re$ | Reynolds number |
| $S$ | Slip ratio |
| $v$ | Velocity (m/s) |
| $X$ | Lockhart–Martinelli parameter |
| $x$ | Flow quality |
| $Z$ | Auxiliar parameter for correlations |
| $z$ | Axial coordinate of pipeline (m) |

*Greek symbols*

| | |
|---|---|
| $\alpha$ | Void fraction |
| $\beta$ | In-situ slippage corrector (Duckler et al. (1964)). |
| $\partial$ | Derivative |
| $\theta$ | Pipeline inclination angle |
| $\lambda$ | Input liquid hold-up |
| $\mu$ | Dynamic viscosity (Pa·s) |
| $\nu$ | Kinematic viscosity (m$^2$/s) |
| $\rho$ | Density (kg/m$^3$) |
| $\sigma$ | Superficial tension (N/m) |
| $\Phi$ | Multiphase multiplier (Lockhart–Martinelli) |

*Subscripts*

| | |
|---|---|
| atm | Atmospheric condition |
| f | Liquid phase indicator |
| g | Gas phase indicator |
| gf | Gas–liquid mixture |
| gm | Gas minus mixture (drift) |
| $i$ | Phase indicator |
| ns | No slip condition |
| o | Inlet condition |

horizontal pipelines by using a new experimental facility which is specifically designed for the analysis of two- and three-phase flows. In this facility transparent methacrylate pipelines and elbows are placed in a sequence of horizontal and vertical orientations (in which the flow has to move sequentially upwards, horizontally, and downwards), so as to measure the influence of the orientation in the flow dynamics. The rig has the capability to regulate and measure the inlet velocities in order to analyze several flow regimes, as well as measure the pressure drop and hold-up in the different segments of the pipeline. Therefore, the current work aims to contribute to a wider scope research, in which reliable database will be generated of two- and three-phase G/L/S mixtures, flowing through horizontal and vertical 30 mm ID pipelines with elbows for different flow regimes. This data will be used to validate correlations as well as CFD simulations. In this first approach, G/L mixtures composed of air and water are analyzed in a horizontal 30 mm ID methacrylate pipeline.

## 2 Gas–liquid correlations

In this section a selection of some relevant correlations for estimating the frictional pressure gradient and void fraction are introduced in detail. Most of the following correlations have been tested by several authors and they have been proven to be reliable. Thus, in order to evaluate the accuracy of the measurements performed, these correlations are then used and compared against data obtained in our experimental facility which is introduced later in Section 3.

### 2.1 Frictional pressure gradient

#### 2.1.1 *Lockhart–Martinelli correlation*

The main insight in Lockhart and Martinelli (1949) correlation was to determine the frictional pressure gradient of the mixture as if each phase were flowing separately in the pipeline. Then these values are corrected by the two phase multipliers, $\Phi_f$ and $\Phi_g$ (Eq. (1)). The assumption is that for each phase, there must be a specific set that includes hydraulic diameter, phase velocity, and friction factor that results in the two-phase frictional pressure gradient. The analysis leads to the postulation that $\Phi_f$ and $\Phi_g$ are functions of the gas and liquid Reynolds numbers and the Lockhart–Martinelli (L–M) parameter $X$, defined in Eq. (3). Empirical curves, meant to be used in design, were obtained from a wide range of experimental data that confirmed the postulation.

$$\left(\frac{\partial P}{\partial z}\right)_{TP} = \Phi_f^2 \cdot \left(\frac{\partial P}{\partial z}\right)_f = \Phi_g^2 \cdot \left(\frac{\partial P}{\partial z}\right)_g \quad (1)$$

$$\Phi_{\mathrm{f}}^2 = f(Re_{\mathrm{f}}, Re_{\mathrm{g}}, X) \tag{2}$$

$$X = \frac{(\partial P / \partial z)_{\mathrm{f}}}{(\partial P / \partial z)_{\mathrm{g}}} \tag{3}$$

### 2.1.2 Chisholm simplification

Chisholm (1967) took Lockhard and Martinelli's work to a deeper level, and proposed a simple equation, for design in engineering, relating the multiphase multipliers with the Lockhart–Martinelli parameter, $X$ (Eq. (4)).

$$\Phi_{\mathrm{f}}^2 = 1 + C / X + 1 / X^2 \tag{4}$$

Here, $C$ is a flow regime indicator. It might adopt four different values regarding the flow mechanism of the phases, as it quantifies to what extent the liquid or gas may flow in a turbulent way ($t$) or in viscous way ($v$).

$$C = \begin{cases} 5, & Re_{\mathrm{f}} < 2000 \text{ and } Re_{\mathrm{g}} < 2000 \,(v-v) \\ 10, & Re_{\mathrm{f}} \geq 2000 \text{ and } Re_{\mathrm{g}} < 2000 \,(t-v) \\ 12, & Re_{\mathrm{f}} < 2000 \text{ and } Re_{\mathrm{g}} \geq 2000 \,(v-t) \\ 20, & Re_{\mathrm{f}} \geq 2000 \text{ and } Re_{\mathrm{g}} \geq 2000 \,(t-t) \end{cases} \tag{5}$$

### 2.1.3 Dukler et al. correlation

Dukler et al. (1964) developed a correlation for predicting the pressure gradient in pipelines. Their study was grounded through the principles of dynamic similarity for two-phase (G/L) flows assuming that kinematic similarity applies to the single phase velocities as it does to the mixture velocities. They found that if dynamic similarity is to exist, then the mixture properties must be defined for the non-slip homogeneous flow:

$$\rho_{\mathrm{ns}} = \rho_{\mathrm{f}} \cdot \lambda + \rho_{\mathrm{g}} \cdot (1-\lambda) \tag{6}$$

$$\mu_{\mathrm{ns}} = \mu_{\mathrm{f}} \cdot \lambda + \mu_{\mathrm{g}} \cdot (1-\lambda) \tag{7}$$

With this, the Reynolds number for the mixture can be calculated as

$$Re_{\mathrm{gf}} = \frac{\rho_{\mathrm{ns}} v_{\mathrm{gf}} D}{\mu_{\mathrm{ns}}} \cdot \beta \tag{8}$$

where $\beta$ corrects the properties from the non-slip condition to the actual slippage of the mixture. It is expressed as

$$\beta = \frac{\rho_{\mathrm{f}} \cdot \lambda^2}{\rho_{\mathrm{ns}} \cdot (1-\overline{\alpha})} + \frac{\rho_{\mathrm{g}} \cdot (1-\lambda)^2}{\rho_{\mathrm{ns}} \cdot \overline{\alpha}} \tag{9}$$

The frictional pressure drop is then calculated as

$$\left(\frac{\partial P}{\partial z}\right)_{\mathrm{gf}} = \frac{\rho_{\mathrm{ns}} v_{\mathrm{M}}^2 f_{\mathrm{f}}}{2D} \cdot \varepsilon(\lambda) \cdot \beta \tag{10}$$

where $\varepsilon(\lambda)$ is the correlation found by Dukler et al. (1964) that represents the ratio between the multiphase friction factor and the single-phase friction factor, given by

$$\varepsilon(\lambda) = \frac{f_{\mathrm{m}}}{f_{\mathrm{f}}} = 1 + \frac{z}{1.281 - 0.478 \cdot z + 0.444 \cdot z^2 - 0.094 \cdot z^3 + 0.00843 \cdot z^4} \tag{11}$$

where $z = -\ln \lambda$.

### 2.1.4 Beggs & Brill correlation

Beggs and Brill (1973) developed a correlation for gas–liquid mixtures flowing in inclined pipes. They observed a lack of reference material to predict the behaviour of gas–liquid mixtures in inclined pipelines together with an increasing number of inclined wells trying to reach for petroleum in unexplored areas. With this in mind they did a large campaign of almost 600 measurements in an experimental rig, studying the effect of 8 parameters: (1) gas flow rate 0–98 m³/s; (2) liquid flow rate 0–1.9 L/s; (3) average system pressure 241–655 kPa; (4) pipe diameter 25.4 and 38.1 mm; (5) liquid hold up 0–0.87%; (6) pressure gradient 0–2.6 Pa/m; (7) inclination angle –90° to +90°; and (8) flow pattern. The equation used to calculate the pressure gradient for any mixture of gas and liquid flowing in a pipeline of internal diameter $D$ and inclination angle $\theta$ is

$$\left(\frac{\partial P}{\partial z}\right)_{\mathrm{gf}} = \frac{\rho_{\mathrm{gf}} \left[ g \cdot \sin\theta + \left( f_{\mathrm{gf}} \cdot v_{\mathrm{gf}}^2 / 2D \right) \right]}{1 - \left[ \left( \rho_{\mathrm{gf}} \cdot v_{\mathrm{gf}} \cdot j_{\mathrm{g}} \right) / P \right]} \tag{12}$$

where $\rho_{\mathrm{gf}}$ is the density of the two-phase mixture:

$$\rho_{\mathrm{gf}} = \rho_{\mathrm{f}} \cdot H_{\mathrm{f}} + \rho_{\mathrm{g}} \cdot (1 - H_{\mathrm{f}}) \tag{13}$$

Equation (12) contains two unknowns: $H_{\mathrm{f}}$ the liquid hold-up used to calculate the in-situ mixture density; and $f_{\mathrm{gf}}$ the friction factor of the mixture to calculate friction losses. In their study, Beggs and Brill proposed correlations for predicting $H_{\mathrm{f}}$ and $f_{\mathrm{gf}}$ from fluid and system properties that are known. First they proposed a method to identify the flow pattern between segregated, intermittent, and distributed. For this $L_1$ and $L_2$ were defined in Eqs. (14) and (15):

$$L_1 = \exp\left(-4.62 - 3.757 \cdot Z - 0.481 \cdot Z^2 - 0.0207 \cdot Z^3\right) \tag{14}$$

$$L_2 = \exp\left(1.061 - 4.602 \cdot Z - 1.609 \cdot Z^2 - 0.179 \cdot Z^3 + 0.635 \times 10^3 \cdot Z^5\right) \tag{15}$$

where $Z$ is a function of the inlet flow rates:

$$Z = \ln\left(\frac{Q_{\mathrm{fo}}}{Q_{\mathrm{fo}} + Q_{\mathrm{go}}}\right) \tag{16}$$

The flow pattern is then identified by comparing the Froude number with the parameters $L_1$ and $L_2$:

if $Fr < L_1$, the flow is segregated;

if $L_1 < Fr < L_2$, the flow is intermittent;

if $Fr > L_1$ and $Fr > L_2$, the flow is distributed.

The friction factor of the two-phase mixture was found to be a function of the input hold-up and the in-situ hold-up:

$$\frac{f_{gf}}{f_{ns}} = f(\lambda / H_f^2) = e^S \tag{17}$$

$$S = \frac{\ln y}{-0.0523 + 3.182 \cdot \ln y - 0.8725 \cdot (\ln y)^2 + 0.01853 \cdot (\ln y)^4} \tag{18}$$

$$y = \frac{\lambda}{H_f^2} \tag{19}$$

Section 2.2.2 will detail the method to calculate $H_f$.

### 2.1.5 Summary of correlations

The correlations for predicting the FPG introduced in Section 2.1 are summarized in Table 1, where only the expression for calculating the FPG is presented for each study together with the reported flow regime applicability.

## 2.2 Void fraction

The void fraction is a very important feature of two-phase flows, as it is directly related with the gas–liquid interface. There are mainly two different approaches available aimed at predicting the void fraction, namely the two-fluid (separate) flow model, and the one dimensional drift flux model. According to Vijayan et al. (2000), the two-fluid flow model can be divided in three groups. The first group is the slip ratio, which uses empirical relations to predict the slip between the phases, the second group uses a corrector factor to adjust homogeneous models, and the last is called miscellaneous correlations, and these are empirical correlations that do not fit in any of the two previous groups.

In this study, some of these correlations are selected and then compared with experimental data. From the two-fluid flow model, the Lockhart and Martinelli, and Beggs and Brill correlations are chosen, while from the drift flux model four correlations have been selected.

**Table 1** Available correlations for the FPG in horizontal gas–liquid two-phase flow

| Literature | $(\partial P / \partial z)_M$ | Flow regime | Section |
|---|---|---|---|
| Lockhart and Martinelli (1949) | $\Phi_i^2 \cdot \left(\frac{\partial P}{\partial z}\right)_i$ | $(v-v);(v-t)$ $(t-v);(t-t)$ | 2.1.1 |
| Chisholm (1967) | $\Phi_i^2 \cdot \left(\frac{\partial P}{\partial z}\right)_i$; $\Phi_f^2 = 1 + C/X + 1/X^2$ | $(v-v);(v-t)$ $(t-v);(t-t)$ | 2.1.2 |
| Dukler et al. (1964) | $\frac{\rho_{ns} v_{gf}^2 f_f}{2D} \cdot \varepsilon(\lambda) \cdot \beta$ | — | 2.1.3 |
| Beggs and Brill (1973) | $\frac{\rho_{gf}\left[g \cdot \sin\theta + \left(f_{gf} \cdot v_{gf}^2 / 2D\right)\right]}{1 - \left[\left(\rho_{gf} \cdot v_{gf} \cdot j_g\right)/P\right]}$ | Segregatted, intermittent, distributed | 2.1.4 |

### 2.2.1 Lockhart–Martinelli void fraction correlation

The Lockhart–Martinelli correlation for void fraction, Eq. (20), is in the group of miscellaneous models, but it is very similar to the models based in the slip ratio model. The slip ratio model correlations are in the form of Eq. (21), and each model specifies an empirical equation for the slip ratio, $S$.

$$\alpha = \left[1 + 0.28(1/x - 1)^{0.64}\left(\rho_g / \rho_l\right)^{0.36}\left(\mu_l / \mu_g\right)^{0.07}\right]^{-1} \tag{20}$$

$$\alpha = \left\{1 + \left[(1-x)/x\right]\left(\rho_g / \rho_f\right)S\right\}^{-1} \tag{21}$$

### 2.2.2 Beggs & Brill

The work of Beggs and Brill (1973) also includes correlations for predicting the liquid hold-up in two-phase flows for all conditions and any inclination angle. Equation (22) determines the liquid hold-up for a pipe inclined $\theta$ degree, where $H_f(0)$, the liquid hold-up for horizontal pipelines, and the coefficient $C$ can be both calculated with equations from Table 2.

$$H_f(\theta) = H_f(0) \cdot \left\{1 + C \cdot \left[\sin(1.8 \cdot \theta) - 1/3 \cdot \sin^3(1.8 \cdot \theta)\right]\right\} \tag{22}$$

### 2.2.3 One-dimensional drift-flux model

The drift flux model was first developed by Zuber and Findlay (1965), and since then several authors have contributed to its development. The model is widely accepted for its simplicity and flexibility over the two-fluid flow model, and it is the prediction approach with more methods proposed to date. The drift flux model determines the void fraction as expressed in Eq. (23):

$$\langle \alpha \rangle = \frac{\langle j_g \rangle}{C_o\left(\langle v_{gf} \rangle\right) + \langle\langle v_{gm} \rangle\rangle} \tag{23}$$

The distribution parameter $C_o$ and the drift velocity $v_{gm}$ are calculated using Eqs. (24) and (25) respectively.

$$C_o = \frac{\langle \alpha \cdot v_{gf} \rangle}{\langle \alpha \rangle \langle v_{gf} \rangle} \tag{24}$$

$$\langle\langle v_{gm} \rangle\rangle = \frac{\langle \alpha \cdot v_{gm} \rangle}{\langle \alpha \rangle} = \frac{\langle \alpha (v_g - v_{gf}) \rangle}{\langle \alpha \rangle} \tag{25}$$

In Eqs. (23)–(25), the angle–angle brackets indicate the

**Table 2** Equations for predicting liquid hold-up

| Flow pattern | Horizontal hold-up | $C$ (upward) | $C$ (downward) |
|---|---|---|---|
| Segregated | $\frac{0.98\cdot\lambda^{0.4846}}{Fr^{0.0868}}$ | $(1-\lambda)\cdot\ln\left(\frac{0.011\cdot Lv^{3.539}}{\lambda^{3.768}\cdot Fr^{1.614}}\right)$ | $(1-\lambda)\cdot\ln\left(\frac{4.7\cdot Lv^{0.1244}}{\lambda^{0.3692}\cdot Fr^{0.5056}}\right)$ |
| Intermittent | $\frac{0.845\cdot\lambda^{0.5351}}{Fr^{0.0173}}$ | $(1-\lambda)\cdot\ln\left(\frac{2.96\cdot\lambda^{0.305}\cdot Fr^{0.0978}}{Lv^{0.4473}}\right)$ | Same as segregated |
| Distributed | $\frac{1.065\cdot\lambda^{0.5824}}{Fr^{0.0609}}$ | 0 | Same as segregated |

$Lv$: Liquid velocity number = $j_f(\rho_f/\rho_g)^{0.25}$.

$Fr$: Froude number = $v_{gf}^2/(gD)$.

cross sectional averaged flow properties and the double angle brackets stand for void weighted cross sectional area averaged flow properties. The distribution parameter accounts for the distribution of the gas phase across the pipe cross section, and the drift velocity is the relative velocity of the gas phase with respect to the two-phase mixture velocity $v_{gf}$. These parameters $C_o$ and $v_{gm}$ have been the focus of several authors in the related literature as they are used to calculate the void fraction. Bhagwat and Ghajar (2014) analyzed several correlations for calculating the distribution parameter and the drift velocity and also proposed a new correlation, and then they compared the performance of the correlations against 8255 experimental data points, where 3845 corresponded to air–water two-phase flow experiments. In Table 3 are listed some of the correlations with the best performance in Bhagwat and Ghajar's study.

According to Eqs. (23)–(25), the one dimensional drift flux model predicts the cross sectional averaged void fraction. However, the equality between the cross sectional and volumetric void fraction is valid for two-component two-phase flow (non-boiling), as in this case the cross sectional distribution of the gas phase with respect to the liquid phase remains invariable over a relatively short length of pipe. Therefore, the void fraction can be expressed in both ways $\langle\alpha\rangle=\alpha$, and with similar arguments, it is applicable for the rest of the quantities in Eqs. (23)–(25).

## 3 Experimental facility

The experimental facility, schematically represented in Fig. 1, is designed to analyze three-phase flows, gas–liquid–solid mixtures (G/L/S), and specifically to reproduce the plug and slug flow regimes in horizontal pipelines and bubbly, slug, churn, and annular flow regimes in vertical pipelines. In this paper, experiments are done for two-phase, gas–liquid mixtures (G/L), in horizontal pipelines.

### 3.1 Experimental setup and test conditions

Generic tap water is used as the liquid phase, and it is stored in a 100 L tank. The water is pumped with a 5.5 kW Weir model AB80 centrifugal slurry pump. The main flow, $j_{f1}$, is measured with an Isoil MS2500 electromagnetic flow meter with an accuracy of ±0.8%, and then delivered to the test section. A secondary flow, $j_{f2}$, is recirculated to the slurry tank with two purposes, (1) to ensure the mixing of the slurry inside the tank, and (2) to be able to measure a wider spectrum of slurry flow rates together with the WEG variable frequency drive (AFD), which controls the slurry pump.

The gas phase is compressed air, taken from the lab manifold at a pressure of 8 bar, previously filtered and dried. The air pressure is then settled at 2 bar for the test section with a pressure reduction valve. The air flow rate is measured using two Omega rotameters with an accuracy of 2% and 3% while being delivered to the test section.

The three-phase test section consists of 30 mm internal diameter (ID) acrylic pipes and is divided in three main sections: "$h$" the horizontal test section (Fig. 2), with a total length of 60 diameters and a previous segment of 110 diameters in order to ensure the complete development of the flow (Fig. 2). "$v1$" the vertical upward test section is connected with section $h$ by a 300 mm of radius elbow and consists of 40 ID and a previous segment of 75 ID. And finally "$v2$" is the vertical downward test section with the same characteristics as section $v1$. The flow visualization is performed in this section with a Photron Mini UX100 fast camera.

An Omega differential pressure transducer is located in section $h$ in order to measure the frictional pressure gradient inside the pipeline. The pressure lines are connected to 5 points of section $h$ so as to measure different segments by arranging a combination of valves. Cautionary measures are taken to avoid air presence in the pressure lines, as it would certainly distort the measurements.

**Table 3** Parameters of the drift flux analysis

| Correlation | Distribution parameter | Drift velocity (m/s) |
|---|---|---|
| Bhagwat and Ghajar (2014)[a] | $\frac{2-(\rho_g/\rho_f)^2}{1+(Re_{gf}/1000)^2}+\frac{\left\{\left\{\sqrt{\left[1+(\rho_g/\rho_f)^2\cos\theta\right]/(1+\cos\theta)}\right\}^{(1-\alpha)}\right\}^{2/5}+C_{0,1}}{1+(1000/Re_{gf})^2}$<br>$C_{0,1}=\left(C_1-C_1\sqrt{\rho_g/\rho_f}\right)\left[(2.6-\beta)^{0.15}-\sqrt{f_{gf}}\right](1-x)^{1.5}$ | $(0.35\sin\theta+0.45\cos\theta)\sqrt{\frac{gD\Delta\rho}{\rho_f}}(1-\alpha)^{0.5}C_2C_3C_4$<br>$C_2=\begin{cases}\left(\frac{0.434}{\log_{10}(\mu_f/0.001)}\right)^{0.15}, & \mu_f/0.001>10\\ 1, & \mu_f/0.001\le 10\end{cases}$<br>$C_3=\begin{cases}(La/0.025)^{0.9}, & La<0.025\\ 1, & La\ge 0.025\end{cases}$<br>$C_4=1$ or $C_4=-1$, if $-50^\circ\le\theta<0^\circ$ and $Fr_{sg}\le 0.1$ |
| Choi et al. (2012) | $\frac{2}{1+(Re_{gf}/1000)^2}+\frac{1.2-0.2\sqrt{\frac{\rho_g}{\rho_f}}\left(1-e^{(-18\alpha)}\right)}{1+(1000/Re_{gf})^2}$ | $0.0246\cos\theta+1.606\left(g\sigma\Delta\rho/\rho_f^2\right)^{0.25}\sin\theta$ |
| Hibiki and Ishii (2003)[b] | (B) $1.2-0.2\sqrt{\rho_g/\rho_f}(1-\exp(-18\alpha))$<br>(S) $1.2-0.2\sqrt{\rho_g/\rho_f}$<br>(A) $1+(1-\alpha)/\left(ha+4\sqrt{\rho_g/\rho_f}\right)$ | (B) $1.41\left(g\sigma\Delta\rho/\rho_f^2\right)^{0.25}(1-\alpha)^{1.75}$<br>(S) $0.35\sqrt{gD\Delta\rho/\rho_f}$<br>(A) $(1-\alpha)/\left\{\alpha+4\frac{\sqrt{\rho_g/\rho_f}\left[\sqrt{gD\Delta\rho(1-\alpha)}\right]}{0.015\rho_g}\right\}$ |
| Gomez (2000) | 1.15 | $1.53\left(g\sigma\Delta\rho/\rho_f^2\right)^{0.25}\sqrt{1-\alpha}\sin\theta$ |

[a] $C_1 = 0.2$ for circular and annular pipes, $C_1 = 0.4$ for rectangular pipes; $\beta = j_g/(j_g+j_f)$; $La=\sqrt{\sigma/(g\Delta\rho)}/D$.

[b] The letters S, B, and A stand for slug flow, bubbly flow, and annular mist, respectively. $\Delta\rho=\rho_f-\rho_g$.

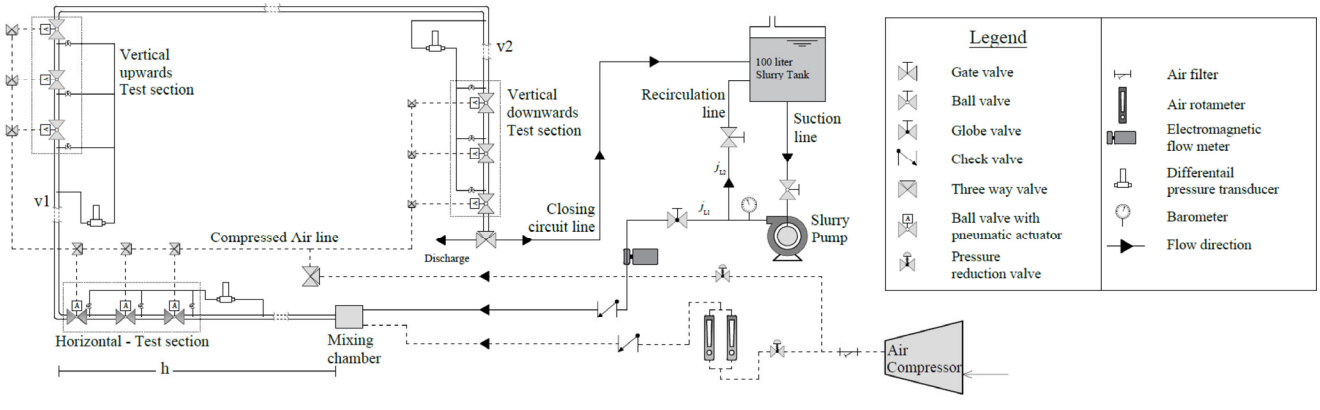


**Fig. 1** Schematic of the experimental facility (not to scale).

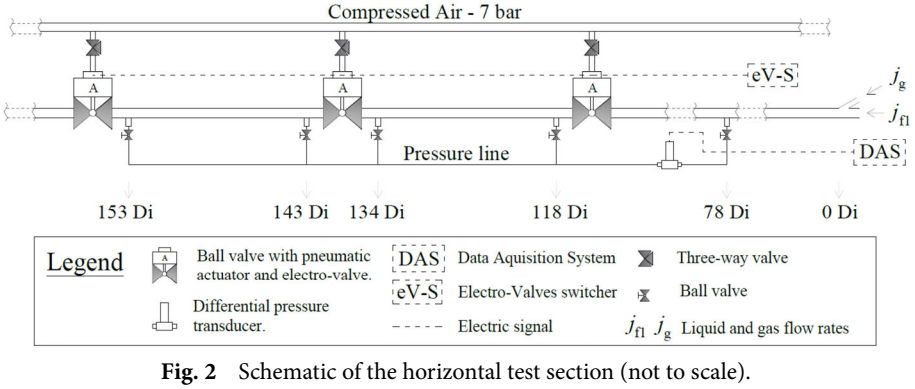


**Fig. 2** Schematic of the horizontal test section (not to scale).

The hold-up is measured by closing simultaneously three quick-closing ball valves with API pneumatic rotary actuators, activated with solenoid valves. The volumetric percentage of each phase trapped between the valves is then measured several times for the same test condition. The valves are full-opening ball valves, with ID equal to the pipe

ID, so that the flow is not disturbed by the valves. A secondary facility provides compressed air at 8 bar to the pneumatic rotary actuators, being capable to fully close the valves simultaneously in 120 ms.

### 3.2 Test conditions

In total, experiments for 25 test conditions are performed in the experimental facility to verify that the measured data is consistent with the literature. The information for the test conditions is summarized in Table 4.

As a first instance, the frictional pressure drop of 9 water one-phase flow rates are measured and compared with the Darcy–Weisbach equation, listed in Table 4 and identified as 1-phase in the "Flow regime" column. Very good agreement is observed among the measurements, and an average percent difference of ±4.5% is obtained. In Fig. 3, the measured data is plotted together with the Darcy–Weisbach curve for frictional pressure drop in a horizontal 30 mm ID smooth pipeline.

**Table 4** Summary of experimental runs

| Run No. | $j_f$ (m/s) | $j_g$ (m/s) | Flow regime | $(\partial P / \partial z)_{fg}$ (kPa/m) | Void fraction |
|---|---|---|---|---|---|
| 1 | 0.84 | 0 | 1-phase | — | — |
| 2 | 1.06 | 0 | 1-phase | — | — |
| 3 | 1.06 | 0.41 | plug | 0.74 | 0.17 |
| 4 | 1.06 | 0.86 | slug | 0.95 | 0.29 |
| 5 | 1.06 | 1.37 | slug | 1.15 | 0.34 |
| 6 | 1.06 | 1.98 | slug | 1.30 | 0.42 |
| 7 | 1.27 | 0 | 1-phase | — | — |
| 8 | 1.41 | 0 | 1-phase | — | — |
| 9 | 1.41 | 0.43 | plug | 1.18 | 0.09 |
| 10 | 1.41 | 0.88 | slug | 1.49 | 0.21 |
| 11 | 1.41 | 1.39 | slug | 1.65 | 0.28 |
| 12 | 1.41 | 2.05 | slug | 1.84 | 0.37 |
| 13 | 1.56 | 0 | 1-phase | — | — |
| 14 | 1.77 | 0 | 1-phase | — | — |
| 15 | 1.77 | 0.44 | plug | 1.71 | 0.07 |
| 16 | 1.77 | 0.95 | slug | 1.97 | 0.18 |
| 17 | 1.77 | 1.47 | slug | 2.30 | 0.20 |
| 18 | 1.77 | 2.10 | slug | 2.60 | 0.26 |
| 19 | 1.98 | 0 | 1-phase | — | — |
| 20 | 1.77 | 2.11 | slug | 2.82 | — |
| 21 | 2.04 | 1.53 | slug | 2.87 | — |
| 22 | 2.12 | 0 | 1-phase | — | — |
| 23 | 2.12 | 0.45 | plug | 2.23 | 0.04 |
| 24 | 2.12 | 1.00 | slug | 2.60 | 0.10 |
| 25 | 2.25 | 0 | 1-phase | — | — |

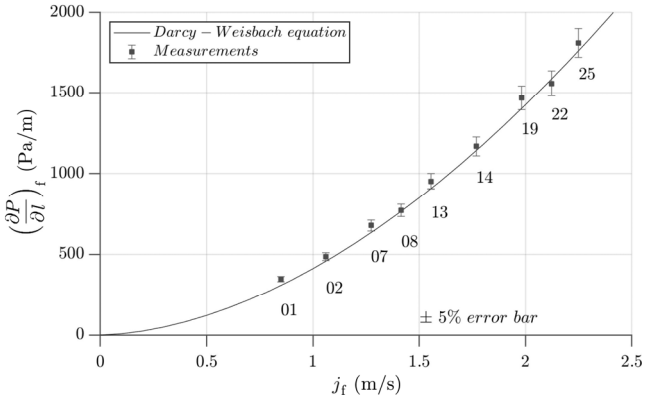


**Fig. 3** Comparison of frictional pressure drop measured and calculated with Darcy–Weisbach equation.

The two-phase flow analysis consists of 16 test conditions with measurements of frictional pressure drop, system pressure, void fraction, and fast camera flow visualization.

To verify the complete development of the flow 5 pressure taps are used to measure pressure drop and plotted in Fig. 4. As it can be seen, the last three measurements are aligned, as expected, and thus the flow is completely developed in the test section.

The void fraction measurements are done by measuring the liquid volume fraction trapped between fast-closing ball valves. As the two-phase flow in plug and slug flow regimes is not homogeneous, at least ten measurements are done for each test condition until a normal distribution of liquid hold-up is obtained. The mean value is then assigned as the void fraction of the test condition.

In order to identify the flow regime, each test condition is visualized with the fast camera. The nose and tail of the long bubbles are analyzed to determine if they correspond to plug or slug bubbles.

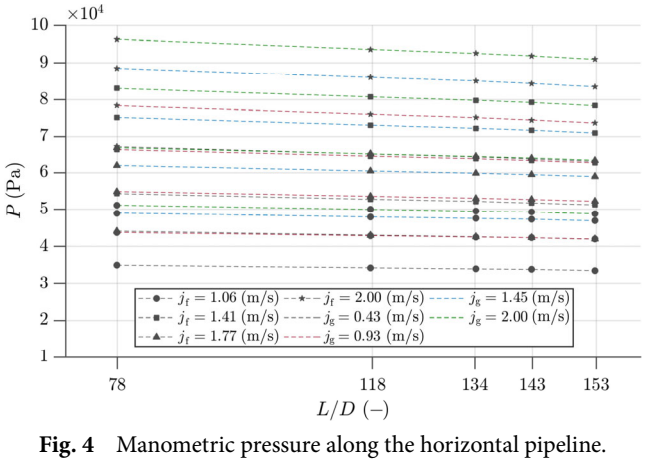


**Fig. 4** Manometric pressure along the horizontal pipeline.

## 4 Results and discussion

The analysis of the test conditions is divided in three sub-

sections: (1) flow regime identification and the comparison against flow regime maps, then (2) frictional pressure drop quantification and evaluation of correlations, and finally (3) the void fraction measurements are compared with correlations to predict it.

In order to evaluate the performance of the different correlations three statistical parameters are used and defined in this section. The averaged percentage difference (APD) between the predicted and measured frictional pressure gradient is defined in Eq. (26), but it is also applicable to others two-phase parameter as the void fraction.

$$\mathrm{APD} = \frac{1}{n}\sum_{k=1}^{n}\left[\frac{(\partial p/\partial z)_{\mathrm{gf,pred}} - (\partial p/\partial z)_{gf,\mathrm{exp}}}{(\partial p/\partial z)_{\mathrm{gf,exp}}}\right]\times 100 \quad (26)$$

With Eq. (26) the over-estimated and under-estimated can be cancelled out, and thus, the average percentage difference is divided into APD(+%) and APD(–%) for over- and under-estimated predictions respectively. Together with the APD, the averaged absolute percentage difference (AAPD) and the root mean square porcentage difference (RMSPD), are also used, defined by Eqs. (27) and (28).

$$\mathrm{AAPD} = \frac{1}{n}\sum_{k=1}^{n}\left|\frac{(\partial p/\partial z)_{\mathrm{gf,pred}} - (\partial p/\partial z)_{\mathrm{gf,exp}}}{(\partial p/\partial z)_{\mathrm{gf,exp}}}\right|\times 100 \quad (27)$$

$$\mathrm{RMSPD} = \sqrt{\frac{1}{n}\sum_{k=1}^{n}\left[\frac{(\partial p/\partial z)_{\mathrm{gf,pred}} - (\partial p/\partial z)_{\mathrm{gf,exp}}}{(\partial p/\partial z) f_{\mathrm{gf,exp}}}\right]^2}\times 100 \quad (28)$$

### 4.1 Flow regime identification

The flow regime is identified using the fast camera. In Fig. 5, it can be seen a plug bubble (Fig. 5(a)) and a slug bubble (Fig. 5(b)). Plug bubbles are smoother and well defined, with very few bubble detachment from the tail or even no detachment from it and inside the air bubble there is no presence of water droplets. On the other hand, slug bubbles (bottom) are much wavier in the interface with many small bubbles around it and detaching from the tail due to the big shear forces in the interface, and there tend to be some water droplets inside the air bubble.

In Fig. 6, the 16 test conditions are plotted in the flow regime map and identified according to the flow regime. It can be seen that the flow transition from plug to slug is in concordance with the Mandhane flow regime map.

### 4.2 Frictional pressure drop

The pressure measurements are plotted in Fig. 4, where it can be seen to what extent the increment of both water and gas flow rates produces an increment on both the system pressure and the slope, this last being the frictional pressure drop. This shows that plug and slug flow regimes are not influenced by one phase, but the two phases contribute to the pressure change. The experimental data obtained from the measurements is then compared with three correlations: (1) Lockhart and Martinelli (L–M), (2) Beggs & Brill (B&B), and (3) Duckler et al. (Dk). In Fig. 7, the performance of the three correlations are plotted together. By plotting the measured values vs. the predicted values it is noticeable how the L–M correlation predicts much better the frictional pressure drop, with an average absolute percent deviation of 10% using the recomended $C$ parameter from the Chisholm simplification, and 6.2% with the fitted value of $C$. The Dk correlation underestimates the pressure drop with very large differences with respect to L–M and B&B, and this is in concordance with the study of Rahman et al. (2013).

The B&B correlation over-estimates the pressure drop; however, for plug flow, the L–M correlation underestimates the frictional pressure drop, while the B&B correlations predicts it within ±10%, as it can be seen in Fig. 7 where the plug flow runs are identified with filled symbols, for both, the Lockhart–Martinelli and Beggs & Brill correlations. The statistical analysis over each correlation is summarized in Table 5.

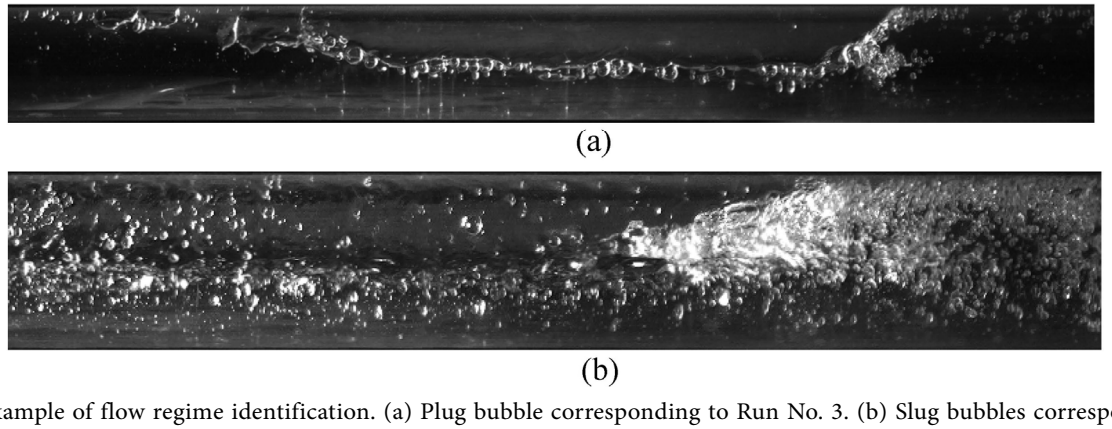


**Fig. 5** Example of flow regime identification. (a) Plug bubble corresponding to Run No. 3. (b) Slug bubbles corresponding to Run No. 18.

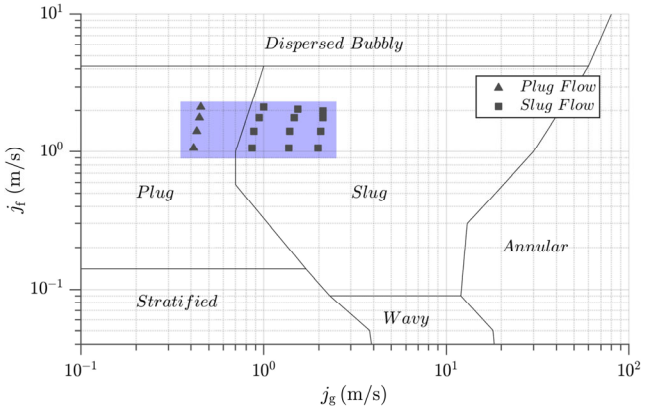


**Fig. 6** Regime map.

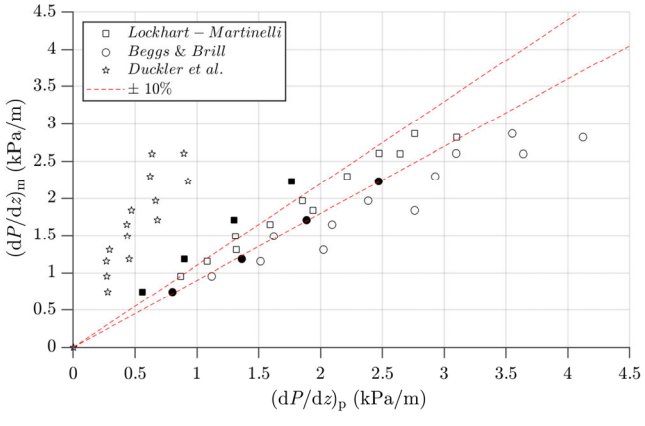


**Fig. 7** Performance of several frictional pressure gradient correlations against experimental data; filled symbols represent plug flow tests.

**Table 5** Performance of tested correlations

| FPG correlation | APD (+%) | APD (−%) | AAPD (%) | RMSPD (%) |
|---|---|---|---|---|
| Lockhart and Martinelli (1949) | | | | |
| • $C = 20$ | 4.5 | 11.9 | 10.0 | 13 |
| • $C = 21$ | 7.8 | 5.7 | 6.2 | 7.3 |
| Beggs and Brill (1973) | 25.7 | — | 25.7 | 29.5 |
| Dukler et al. (1964) | — | 69 | 69.1 | 69.4 |
| $\Phi_l = 1 + C / X + 1 / X$ | | | | |
| $C = 20$ | 2.2 | 4.0 | 3.5 | 4.0 |
| $C = 25$ | 5.4 | 2.2 | 4.4 | 5.5 |
| $C$ = fitted | 3.8 | 2.9 | 3.2 | 3.7 |

When applying the Chisholm simplification to the Lockhart–Martinelli correlation, the correct value of the parameter $C$, from Eq. (4), must be chosen according to the gas and liquid Reynolds numbers. Chisholm (1967) proposed a value of $C$ = 20 for mixtures flowing in turbulent–turbulent regime. In Fig. 8, the multiphase multiplier, $\Phi_l$, calculated with the experimental data, is plotted against the

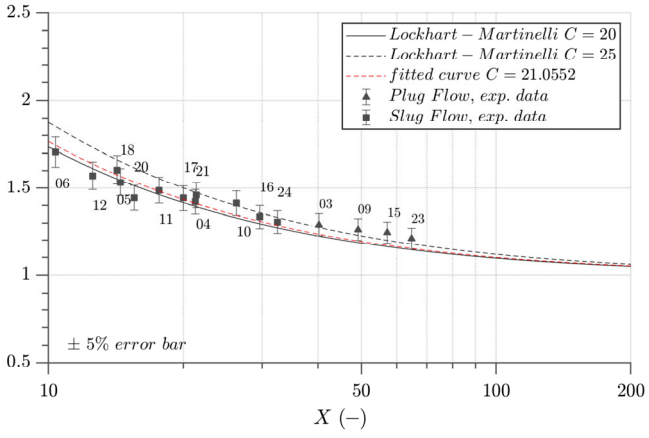


**Fig. 8** Multiphase mutltiplier against Lockhard–Martinelli parameter.

Lockhart and Martinelli parameter ($X$), together with the curves for predicting the multiphase multiplier with values of $C$ = 20 and $C$ = 25, as this last value was suggested by Talley et al. (2015) and Kong et al. (2017). The red dashed curve is the fitted curve for the present experimental data, and corresponds to a curve with $C$ = 21. The average absolute disagreement of the experimental data for $C$ = 20, $C$ = 25, and $C$ = 21 are 3.5%, 4.4%, and 3.2%, respectively, as listed in Table 5 together with the rest of the statistical parameters. It can be noted that for slug flow, larger values of the multiplier are obtained; this means that the increment of the gas flow rate has a big impact in the pressure drop. The two-phase pressure drop is calculated as the product of the multiphase multiplier and the frictional pressure drop of the liquid phase, as indicated in Eq. (1).

Note that the value of the parameter $C$ is obtained by fitting experimental data for plug and slug flows. According to Chisholm (1967), the same value of the parameter is applicable for other turbulent–turbulent regimes, as bubbly or annular flows. On the other hand, for stratified flows, which correspond to viscous regimes, the use of the correlation needs lower values of $C$. Kong et al. (2018) reported experimental data for plug, slug, and bubbly flows for two different pipe sizes, comparing the data with the Chisholm simplification with $C$ = 20 these authors obtained an average percent difference of ±2.8% in the whole range.

## 4.3 Void fraction

The void fraction measurements are also compared with the correlations of Section 2.2, assuming that $\langle \alpha \rangle = \alpha$ for two-component two-phase flows. It can be seen in Fig. 9 that the performance of the predictions against the measured void fraction. The best agreement is achieved by the Lockhart–Martinelli correlation. It can also be seen that the void fraction prediction methods of the drift flux analysis they all perform similarly, with slight differences between them.

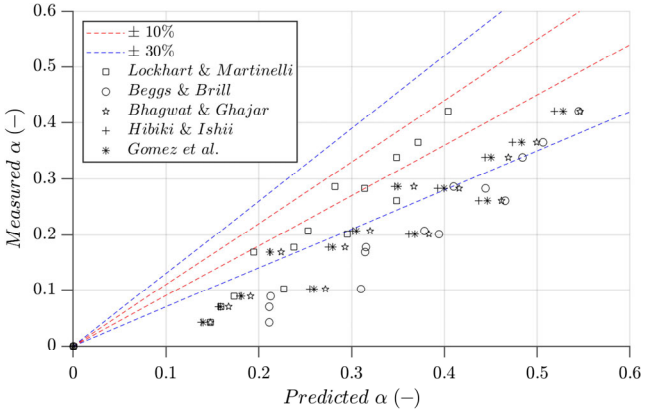


**Fig. 9** Performance of several void fraction correlations against experimental data.

## 5 Conclusions

A new experimental facility was introduced, and measurements of plug and slug flow regimes were carried out for air–water two-phase flow. The flow regime, pressure drop, and void fraction obtained from the measurements were compared with the regime map and several correlations available in the literature. The results shown in Section 4 were generally in concordance with the previous studies. The flow regime transition from plug to slug flow agreed with the flow regime map from the literature. The results presented in this study correspond to plug and slug air–water two-phase flows, in turbulent–turbulent flow regime according the characterization proposed by Lockhart and Martinelli (1949). Future experimental campaigns will consider annular and bubbly flows in order to encompass a wider operational range.

Three correlations for predicting the frictional pressure drop were used and their performance was compared. It was found that the Lockhart and Martinelli correlation gives the best prediction with an average absolute percentage difference (AAPD) of 6.2% when using the Chisholm simplification with the parameter $C$ calculated by fitting the experimental data. Although for low values of gas flow rate the Beggs and Brill correlation predicts the frictional pressure gradient with better results

Several correlations were performed and compared in order to predict the void fraction including the one dimensional drift flux analysis, using correlations to calculate the drift flux parameters from different authors. It was found that the drift flux analysis over-estimates the predicted void fraction, obtaining similar results for the different correlations. The best prediction was achieved by the Lockhart and Martinelli void fraction correlation.

The main objective of the experimental facility introduced in this paper is to analyze three-phase (G/L/S) flows. However, a first approach in two-phase flows was required to compare the measurements and warrant its accuracy. The authors consider that the results obtained in air–water two-phase flow are accurate, and thus three-phase (G/L/S) flows are expected to perform well in the introduced facility.

## Aknowledgements

This project has received funding from the European Union's Horizon 2020 research and innovation programme under the Marie Sklodowska-Curie grant agreement No. 713679; from the Spanish government under the grant DPI2016-75791-C2-1-P; and from Generalitat de Catalunya under grant 2017-SGR-01234. These supports are gratefully acknowledged. We also appreciate the great help of the lab technician, Jordi Iglesias.

## References

Abduvayt, P., Arihara, N., Manabe, R., Ikeda, K. 2003. Experimental and modeling studies for gas–liquid two-phase flow at high pressure conditions. *J Jpn Petrol Inst*, 46: 111–125.

Beggs, D. H., Brill, J. P. 1973. A study of two-phase flow in inclined pipes. *J Petrol Technol*, 25: 607–617.

Bhagwat, S. M., Ghajar, A. J. 2014. A flow pattern independent drift flux model based void fraction correlation for a wide range of gas–liquid two phase flow. *Int J Multiphase Flow*, 59: 186–205.

Chisholm, D. 1967. A theoretical basis for the Lockhart–Martinelli correlation for two-phase flow. *Int J Heat Mass Tran*, 10: 1767–1778.

Choi, J., Pereyra, E., Sarica, C., Park, C., Kang, J. 2012. An efficient drift-flux closure relationship to estimate liquid holdups of gas–liquid two-phase flow in pipes. *Energies*, 5: 5294–5306.

Dukler, A. E., Wicks, M., Cleveland, R. G. 1964. Frictional pressure drop in two-phase flow: B. An approach through similarity analysis. *AIChE J*, 10: 44–51.

Gomez, L. E., Shoham, O., Schmidt, Z., Chokshi, R. N., Northug, T. 2000. Unified mechanistic model for steady-state two-phase flow: Horizontal to vertical upward flow. *SPE J*, 5: 339–350.

Hibiki, T., Ishii, M. 2003. One-dimensional drift-flux model and constitutive equations for relative motion between phases in various two-phase flow regimes. *Int J Heat Mass Tran*, 46: 4935–4948.

Kong, R., Kim, S., Bajorek, S., Tien, K., Hoxie, C. 2017. Experimental investigation of horizontal air–water bubbly-to-plug and bubbly-to-slug transition flows in a 3.81 cm ID pipe. *Int J Multiphase Flow*, 94: 137–155.

Kong, R., Kim, S., Bajorek, S., Tien, K., Hoxie, C. 2018. Effects of pipe size on horizontal two-phase flow: Flow regimes, pressure drop, two-phase flow parameters, and drift-flux analysis. *Exp Therm Fluid Sci*, 96: 75–89.

Lockhart, R. W., Martinelli, R. C. 1949. Proposed correlation of data for isothermal two-phase, two-component flow in pipes. *Chem Eng Prog*, 45: 39–48.

Mandhane, J. M., Gregory, G. A., Aziz, K. 1974. A flow pattern map for gas–liquid flow in horizontal pipes. *Int J Multiphase Flow*, 1: 537–553.

Mao, F., Desir, F. K., Ebadian, M. A. 1997. Pressure drop measurement and correlation for three-phase flow of simulated nuclear waste in a horizontal pipe. *Int J Multiphase Flow*, 23: 397–402.

Rahman, M. A., Adane, K. F., Sanders, R. S. 2013. An improved method for applying the Lockhart–Martinelli correlation to three-phase gas–liquid–solid horizontal pipeline flows. *Can J Chem Eng*, 91: 1372–1382.

Taitel, Y., Dukler, A. E. 1976. A model for predicting flow regime transitions in horizontal and near horizontal gas–liquid flow. *AIChE J*, 22: 47–55.

Talley, J. D., Worosz, T., Kim, S. 2015. Characterization of horizontal air–water two-phase flow in a round pipe part II: Measurement of local two-phase parameters in bubbly flow. *Int J Multiphase Flow*, 76: 223–236.

Vijayan, P. K., Patil, A. P., Pilkhwal, D. S., Saha, D., Venkat Raj, V. 2000. An assessment of pressure drop and void fraction correlations with data from two-phase natural circulation loops. *Heat Mass Transfer*, 36: 541–548.

Zuber, N., Findlay, J. A. 1965. Average volumetric concentration in two-phase flow systems. *J Heat Transf*, 87: 453–468.